RNA Imaging

DOI: 10.1002/anie.201406022

Brightness through Local Constraint—LNA-Enhanced FIT Hybridization Probes for In Vivo Ribonucleotide Particle Tracking**

*Felix Hövelmann, Imre Gaspar, Simon Loibl, Eugeny A. Ermilov, Beate Röder, Jesper Wengel, Anne Ephrussi, and Oliver Seitz**

Abstract: *Imaging the dynamics of RNA in living cells is usually performed by means of transgenic approaches that require modification of RNA targets and cells. Fluorogenic hybridization probes would also allow the analysis of wild-type organisms. We developed nuclease-resistant DNA forced intercalation (FIT) probes that combine the high enhancement of fluorescence upon hybridization with the high brightness required to allow tracking of individual ribonucleotide particles (RNPs). In our design, a single thiazole orange (TO) intercalator dye is linked as a nucleobase surrogate and an adjacent locked nucleic acid (LNA) unit serves to introduce a local constraint. This closes fluorescence decay channels and thereby increases the brightness of the probe–target duplexes. As few as two probes were sufficient to enable the tracking of oskar mRNPs in wild-type living Drosophila melanogaster oocytes.*

One of the important goals in cell and developmental biology is to visualize and track the dynamics of RNA and ribonucleotide particles (RNPs) in living cells.[1] The need for RNA imaging methods has fueled the development of nucleic acid based probes that fluoresce upon hybridization with the targeted RNA molecule.[2] Fluorescent probes useful for live-cell RNA imaging must provide 1) high fluorescence enhancement in the presence of the specific target, to distinguish bound from unbound states, 2) intracellular stability, which is achieved by modified DNA/RNA building blocks, and 3) high brightness to enable the unequivocal, above-noise detection of targets at low local concentration with high spatial resolution.

The first two criteria are met by 2′O-Me-RNA-modified molecular beacons (MBs), reactive probes, and forced intercalation (FIT) probes (Figure 1 A).[3] However, when individual RNPs are to be resolved, brightness becomes the limiting factor. This is the main reason why RNP imaging usually has been performed by means of transgenic approaches. This involves the tagging of RNA with repeat sequences and co-expression of fluorescent fusion proteins that recognize the RNA tags.[4] For example, the MS2-fluorescent protein (MS2–FP) system is often used because dozens of fluorophores per RNA molecule provide high brightness (Figure 1 B).[5] However, the RNA tag insertion may lead to aberrant RNA structure and its artificial expression may perturb the dynamics of RNP biogenesis. By contrast, chemically synthesized fluorescent or fluorogenic probes provide the means to detect endogenous, nonaltered RNA molecules. More importantly, perhaps, in organisms with no or limited transgenesis, chemical probes may be the sole source of information on RNP dynamics.

We envisioned that a small number (≤ 5) of short (< 20 nucleotides (nt)) and very bright fluorogenic probes directed against different segments of the RNA target should provide a signal that enables resolution of cell-endogenous RNPs (Figure 1 C). Conventional MB probes rely on a con-

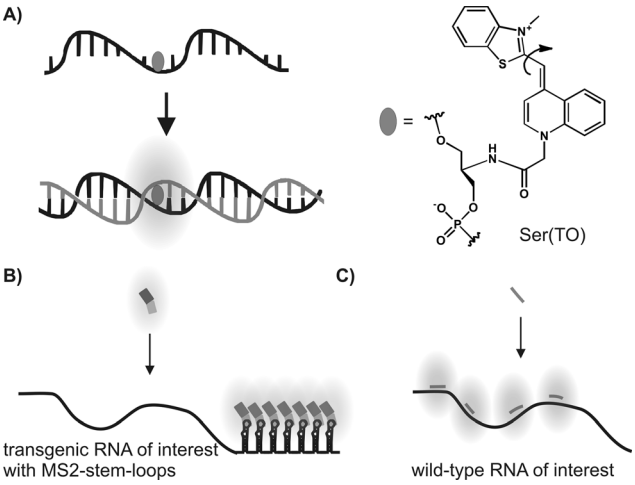

Figure 1. A) FIT probes and the structure of thiazole orange Ser(TO) nucleotide. Principle of live-cell imaging of B) stem-loop-tagged RNA with GFP-MS2 coat proteins or C) wild-type RNA with multiple FIT probes.

[*] F. Hövelmann,[+] S. Loibl, Prof. Dr. O. Seitz
Department of Chemistry, Humboldt-Universität zu Berlin
Brook-Taylor-Strasse 2, 12489 Berlin (Germany)
E-mail: oliver.seitz@chemie.hu-berlin.de
Dr. I. Gaspar,[+] Dr. A. Ephrussi
European Molecular Biology Laboratory
Meyerhofstrasse 1, 69117 Heidelberg (Germany)
Dr. E. A. Ermilov, Prof. Dr. B. Röder
Department of Physics, Humboldt University Berlin
Newtonstrasse 15, 12489 Berlin (Germany)
Prof. Dr. J. Wengel
Department of Physics, Chemistry and Pharmacolog
University of Southern Denmark Odense
Campusvej 55, 5230 Odense M (Denmark)
[+] These authors contributed equally to this work.
[**] This work was supported by the Deutsche Forschungsgemeinschaft and the European Molecular Biology Laboratory. LNA = locked nucleic acid, FIT = forced intercalation.
Supporting information for this article is available on the WWW under http://dx.doi.org/10.1002/anie.201406022.

formational change between a fluorophore and a quencher.[6] This change can also be caused by unintended yet difficult to avoid binding to proteins.[7] Furthermore, residual quenching in the target-bound state limits MB brightness. We recently reported quencher-free FIT probes (Figure 1A).[8] In these probes, a dye of the thiazole orange (TO) family is linked as a base surrogate. Single-stranded FIT probes show low fluorescence. Hybridization with the RNA target forces the dye to intercalate, which results in an increase of TO fluorescence.[9] To enhance the brightness of FIT probes, we recently combined the highly responsive TO with its extremely bright emitting oxazolopyridine-based relative JO.[10] Though highly successful in wash-free FISH protocols, JO proved to be too labile to be used in chemically modified, nuclease-resistant probes required for live-cell imaging.

In pursuit of bright hybridization probes for live-cell RNP imaging, we reconsidered the FIT probe design. Excitation of the TO dye induces twisting around the methine bridge, which depletes the excited state of TO in low-viscosity environments.[11] Hybridization forces the dye to arrange within the double-helical base stack. This high-viscosity environment impedes twisting motions.[12] The resulting increase of the excited state lifetime leads to an increase of the fluorescence quantum yield. We inferred that the brightness of the target-bound FIT probes can be improved by increasing the viscosity in the TO vicinity and we assumed that this can be achieved through the introduction of a local constraint. In DNA–RNA duplexes, the RNA strand adopts an A-type conformation, while the DNA strand is less clearly defined.[13] NMR studies,[14] MD simulations,[15] and measurements of charge transfer[16] suggested that locked nucleic acid (LNA) modifications rigidify the A-type structure within the DNA moiety because the sugar pucker is locked in the C3′-*endo* conformation (Figure 2).[17] We assumed that the increase in rigidity and the accompanying decrease in helical rise per base pair introduced by LNA should reduce the volume available for twisting motions around the methine bridge of the adjacent TO nucleotide and, thereby, increase the quantum yield of TO emission.

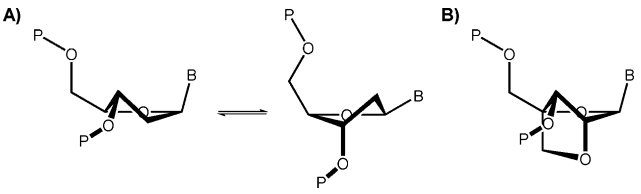

Figure 2. A) In nucleic acid duplexes, 2′-deoxyribonucleotides can adopt C3′-*endo* (left) and C2′-*endo* (right) conformations. B) LNA conformation is fixed in the C3′-*endo* pucker.

To test the hypothesis, the LNA modification was introduced at various positions in a DNA FIT probe directed against a segment of neuraminidase mRNA of H1N1 influenza (Figure 3A). We measured UV/Vis and fluorescence spectra before and after addition of target RNA. The LNA monomer increased the fluorescence quantum yield by 17–152% when placed next to the TO nucleotide (shaded area in Figure 3A). Both single-stranded and target-bound probes were affected, and the fluorescence enhancement upon hybridization was not significantly altered unless several LNA monomers were introduced. The "LNA effect" vanished when LNA and TO were separated by one or more nucleotides. This suggested that the fluorescence enhancement induced by the LNA nucleotide was due to a local constraint.

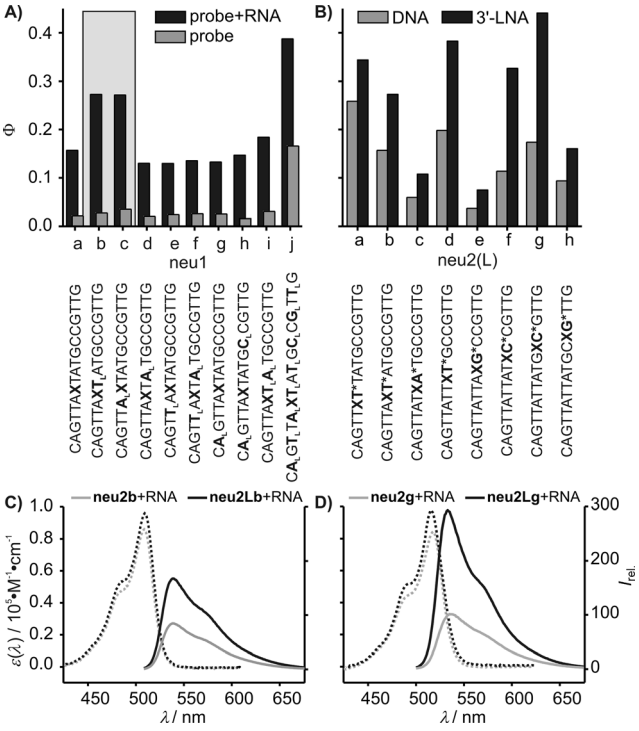

Figure 3. Comparison of quantum yields A) before (gray) and after (black) hybridization with RNA target CAACGGCAUAAUAACUG; B) in target-bound state of FIT probes. C,D) Absorbance (dashed) and fluorescence emission (solid) spectra in target-bound state of DNA only (gray, N* = dN) and LNA-enhanced probes (black, $N^* = N_L$). Conditions: 0.5 μM probe and 5 equiv RNA target (when added) in PBS (100 mM NaCl, 10 mM Na_2HPO_4, pH 7), 37 °C; $\lambda_{ex} = 485$ nm, $\lambda_{em} = 500$–700 nm. (X = Ser(TO), subscript L marks LNA nucleotides.

We assessed the robustness of the "LNA effect" by placing dinucleotides comprising a TO nucleotide and an adjacent LNA nucleotide at eight different positions of the 17-mer oligonucleotide (Figure 3B). As observed previously, TO emission was dependent on the sequence context.[10] Yet, the comparison with the corresponding TO-only walk revealed that, in each case, the LNA provided an increase in fluorescence quantum yield (30–187%).

The optical properties of three DNA FIT probes were studied in greater detail (Table 1; Table S1). UV/Vis measurements showed that the introduction of a neighboring LNA monomer in **neu2Lb**, **neu2Ld**, and **neu2Lg** probes resulted in a 12–21% increase of the TO absorbance both in single-stranded and target-bound states, reaching a remarkable value of $98000\,M^{-1}cm^{-1}$. This is 56% higher than the absorbance of unconjugated TO.[18] The underlying phenomenon causing this increase of absorbance is still unclear, but it seems plausible to assume that the LNA modification fosters

Table 1: Fluorescence lifetime, extinction coefficient, and quantum yield of DNA and LNA-modified FIT probes.

ON	τ (a)[a]				ε_{max}[b]	Φ[c]
	very fast	fast	medium	slow		
neu2b	0.047 (43)	0.29 (37)	1.00 (16)	3.16 (4)	82260	0.02
neu2Lb	0.040 (42)	0.27 (37)	1.00 (15)	3.31 (6)	92620	0.02
neu2b + RNA	–	0.23 (25)	1.22 (33)	3.15 (42)	86320	0.16
neu2Lb + RNA	–	–	0.99 (31)	3.53 (69)	96350	0.27
neu2d	0.055 (37)	0.38 (34)	1.20 (23)	2.70 (6)	79520	0.05
neu2Ld	0.080 (20)	0.49 (41)	1.30 (29)	3.20 (10)	95330	0.07
neu2d + RNA	–	–	0.99 (33)	2.85 (67)	79530	0.20
neu2Ld + RNA	–	–	1.50 (20)	3.64 (80)	96250	0.38
neu2g	0.050 (28)	0.40 (37)	1.00 (29)	2.70 (6)	83080	0.04
neu2Lg	–	0.13 (14)	1.36 (45)	2.55 (41)	96100	0.14
neu2g + RNA	–	–	0.94 (28)	2.96 (72)	85020	0.21
neu2Lg + RNA	–	–	1.00 (6)	4.15 (94)	98430	0.44

[a] τ = fluorescence decay lifetimes [ns]; relative amplitudes a in the emission decay fits are given in parentheses. [b] Molar extinction coefficient [$M^{-1}cm^{-1}$] at absorption maxima (513–518 nm). [c] Quantum yield.

ground-state interactions between TO and the adjacent nucleobases.

To characterize the influence of LNA on the TO excited state, fluorescence lifetimes (Table 1; Table S1 and Figure S1) were measured.[18] The four processes governing decay were categorized as very fast (0.04–0.08 ns), fast (0.13–0.49 ns), medium (0.99–1.59 ns), and slow decays (2.13–4.15 ns). Hybridization closed decay channels correlated with the fast decay processes. The LNA modification had a remarkable effect on the slow decay process of target-bound FIT probes: its amplitude was increased from a mean of 60% to 81% in LNA FIT probes at the expense of the medium decay (Table 1, Table S1). Furthermore, the decay times of the slow process were extended from 2.99 ns to 3.73 ns on average. This resulted in increased fluorescence lifetimes for LNA-containing FIT probes, which correlated with the observed enhancement of the fluorescence quantum yields. The data from UV absorbance, steady-state fluorescence, and time-resolved fluorescence studies likely reflects the previously reported increase of rigidity around the LNA modification, which probably fosters TO–nucleobase interactions and, thereby, helps shut down decay channels opened by TO twisting motions.

We designed a set of hybridization probes for imaging *oskar* mRNA-containing RNPs in developing oocytes of *Drosophila melanogaster* (Table 2).[19] To prevent cleavage of target RNA by RNase H, four LNA nucleotides were introduced. The resulting probe **osk1b** showed very bright emission upon hybridization with target RNA in vitro. However, the stability against DNase I digestion was low and in vivo the fluorescence signal faded away within 45 min (Table S2, Figure S2). Of note, degradation of FIT probes did not result in false positive signals, which would be observed when molecular-beacon-like probes are enzymatically degraded (a comparison between FIT and MB probes is shown in Ref. [9b]). The fully 2′-O-Me-modified FIT probe **osk1c** showed increased stability against DNase I, but hybridization-induced enhancement and brightness of TO emission were severely reduced. Introduction of a single LNA modification next to the TO nucleotide restored the responsiveness of the multi-*O*-Me-RNA probe **osk1d**. Optimal stability and desirable fluorescence properties were obtained by leaving a 1 nt gap between the TO–LNA dinucleotide and the 2′-O-Me segments (Figures S2 and S3, Table S2).

The 1 nt gap design was applied to other probes (**osk2–6**) targeted against different segments of *D. melanogaster oskar* mRNA (Table 2; Tables S4 and S5). Targets of the **osk1–5** probes were chosen for their distribution along the RNA, potential interference with known protein binding sites and RNA secondary structure was avoided. With this set we assessed the utility of LNA-enhanced FIT probes for live-cell imaging in comparison with the *osk*MS2-(10x)–GFP system.[20] We compared the overall background-corrected signal-to- noise ratio (SNR, reports normalized brightness of injected probes/probe mixtures) and the signal-to-background ratio (SBR or contrast); these two key parameters determine the detection of particle-like features (PLFs) in the images (Figure S4).

We found that injecting a single FIT probe was sufficient to detect RNA localized at the posterior pole. However, lower amounts of RNA, particularly moving RNPs distributed throughout the egg chamber, were not resolved, which hampers particle tracking (Movie S1). To enable the unambiguous detection of *oskar* transport particles containing low amounts of *oskar* mRNA, we injected (1–4% of oocyte volume) combinations of different gapmer FIT probes at 5–45 μM concentration. Direct comparison of signal intensities and SBR with those of the *osk*MS2–GFP system revealed that a mixture of 3–4 probes on average exhibit a fluorescence similar to that of the ten GFP molecules labeling a single *osk*MS2(10x) mRNA (Figure 4 A′, A″, and B). Due to the similar fluorescence properties of TO and GFP, this might indicate that most of the detected RNPs contain a comparable amount of MS2-labeled and endogenous *oskar* as a result of mRNA oligomerization.[21] SBR provided by these injected mixtures was substantially lower than that of the *osk*MS2 system (Figure 4 B and Figure S4E), where the unbound GFP is contained in the distant nuclei of the nurse cells. Reducing

Table 2: Comparison of DNA, LNA, 2′-O-Me and gapmer FIT-probes targeted against *oskar* mRNA.

ON	Sequence[a]	Φ	Φ/Φ_0	Br[b]
osk1a	$_{83}$GACTTAAGATAXTAGGTTTTGGCG$_{106}$	0.22	11.7	9.7
osk1b	T$_L$AAG$_L$ATAXT$_L$AGGT$_L$T	0.36	13.4	16.4
osk1c	GACTTAAGATAXTAGGTTTTGGCG	0.12	4.2	4.9
osk1d	TTAAGATAXT$_L$AGGTTTTGG	0.34	13.2	16.6
osk2	$_{2642}$GCGGAAAAGXT$_L$TGAAGAGA$_{2616}$	0.40	7.6	19.7
osk3	$_{2229}$CTCGTTTCAATAACXT$_L$GCA$_{2211}$	0.28	4.3	14.1
osk4	$_{1462}$ACCGATXT$_L$TGTTCCAGAAC$_{1444}$	0.28	5.8	13.1
osk5	$_{2197}$CGGTTTTCTGGXT$_L$TTGGGT$_{2179}$	0.43	8.0	21.2
osk6	$_{822}$GTCAGXT$_L$TTCGATATTCAC$_{804}$	0.42	6.1	21.1

[a] Underlined letters represent 2′-O-Me nucleotides; subscript "L" represents LNA nucleotides and X denotes Ser(TO); numbers in subscript indicate the position of the target segment in *oskar* mRNA. [b] Br = brightness in $mL\,mol^{-1}\,cm^{-1}$.

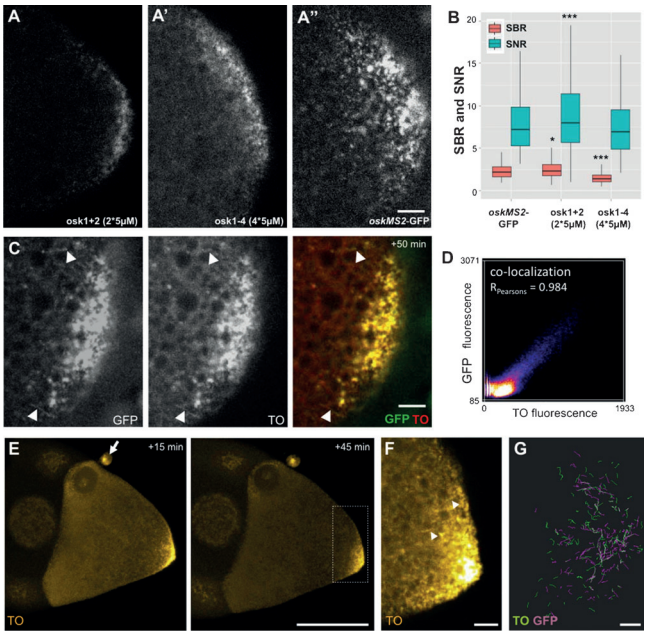

Figure 4. A) Confocal microscopy images of wild-type (w^{1118}) oocytes 15 min after injection of FIT probes (A, A′) and of an uninjected oocyte expressing *osk*MS2–GFP (A″). B) Optical properties of PLFs. C and F) Time projection of ten successive frames of an *osk*MS2–GFP-expressing oocyte and a wild-type oocyte (Movies S2 and S3, 1.6 frames per second), respectively, injected with a mixture of **osk1**+**2**+**4** (15 μM each). Images were recorded close to the posterior pole (see E). Arrowheads indicate moving *oskar* RNPs. D) Colocalization of GFP and TO fluorescence in panel C. E) Wild-type oocyte 15 and 45 min after injection. G) Merge of *oskar* RNP trajectories obtained with the oskMS2–GFP system (magenta) and with **osk1**+**2**+**4** (green) from six oocytes. Overlapping tracks appear in white. Conditions: (A–A′, E, F) λ_{ex} = 514 nm, λ_{em} = 525–625 nm, (A″) λ_{ex} = 488 nm, λ_{em} = 500–600 nm. (C) TO: λ_{ex} = 525 nm, λ_{em} = 535–625 nm, GFP: λ_{ex} = 470 nm, λ_{em} = 480–520 nm. Scale bars represent 5 μm (A, C, F, and G) and 50 μm (E).

Table 3: Motility parameters of *oskar* RNPs tracked by MCP–GFP or by injected FIT probes.[a]

Genotype conditions	*osk*MS2 non-injected	*osk*MS2 injected	*osk*MS2 injected	w^{1118} injected
label	GFP	GFP[b]	TO[b]	TO
tracks/oocytes	133/4	158/6	139/6	238/11
motile fraction [%][c]	23.4 ± 2.5	23.1 ± 2.7	22.8 ± 2.5	20.2 ± 2.3
Displacement[d] [μm]	1.78 ± 1.31	1.82 ± 1.11	1.67 ± 0.98	1.80 ± 1.06
duration[d] [s]	4.80 ± 3.65	5.26 ± 3.66	4.1 ± 3.25*	5.02 ± 3.92
speed[d] [μm s^{-1}]	0.39 ± 0.01	0.38 ± 0.01	0.45 ± 0.01*	0.40 ± 0.01

[a] A mixture of osk-1 + 2 + 4 (15 μM each) was microinjected into stage 9 oskMS2–GFP and wild-type (w1118) oocytes and assayed 35–45 min after injection. [b] GFP and TO signals from the same oskMS2–GFP oocytes. [c] Mean ± SEM. [d] Mean ± SD. * significant difference ($p < 0.05$) when compared to uninjected oskMS2–GFP oocytes.

the number of different probes to two (Figure 4A) greatly decreased the background and thus improved the SBR to the point that it slightly exceeded that of *osk*MS2–GFP (Figure 4B).[22] To directly compare FIT probes to *osk*MS2-GFP, we injected mixtures of 2–4 probes into *osk*MS2–GFP-expressing oocytes. Despite suboptimal spectral detection settings (see Figure 4 legend), we observed near-perfect correlation between the two signals (Figure 4C,D and Movie S2).

Computer-assisted particle tracking was used to analyze *oskar* RNP motility.[23] We found that the major motility parameters determined by the TO channel were nearly indistinguishable from the parameters revealed by the GFP channel in both injected oocytes and non-injected reference oocytes, regardless of the number of probes used in the mixture (Table 3 and Figure S5E–G). The fraction of motile particles and the displacements were identical. Of note, despite analysis of the same specimen and the high degree of colocalization, we observed only about 40% overlap when tracking GFP and TO signals in the injected *osk*MS2–GFP oocytes (Figure 4G). This and the almost identical number of collected tracks (Table 3) suggest that although a large fraction of GFP-positive RNPs was not captured in the TO channel—probably because of the suboptimal, 525 nm excitation required to spectrally resolve GFP from TO emission—the FIT probes stained numerous endogenous mRNA-containing RNPs that were not detected by the MS2–GFP system. The difference in number of "labeled RNA molecules" might explain the similar brightness of 10xGFP and 3–4 FIT probes.

LNA-enhanced FIT probes were used to image RNP motility in wild-type oocytes that did not express *osk*MS2–GFP (Figure 4E,F; Movie S3). Using 3–4 LNA-enhanced gapmer FIT probes in the injection mixture at an initial concentration of 40–45 μM, we observed an almost identical number and a similar distribution of *oskar* particles within the oocytes as in the uninjected GFP control (Figure S5A).[24] Most importantly, we found no striking difference in *oskar* RNP motility (Table 3; Figure S5E–G). These findings indicate that LNA gapmer probes are valid tools to study mRNP behavior in vivo.

Hybridization probes have been utilized previously to analyze RNP trafficking in vivo. Mhlanga and co-workers injected four MB probes and reported that *oskar* mRNA is transported in large RNPs containing several hundreds of mRNA molecules.[25] These large RNPs showed about tenfold reduced motility compared to RNPs revealed by the *osk*MS2–GFP system.[20,23] Such large granules of nonlocalized *oskar* mRNA are observed in egg chambers under nutrition-deprivation stress.[26] Thus, it seems crucial for RNP imaging to carefully explore the conditions under which exogenous nucleic acids are applied to target endogenously expressed RNA.

It is obviously important to avoid probe-mediated interference with physiological RNP biogenesis. On the other hand, targeted disruptions might be powerful tools for deciphering the function of RNA secondary structures or protein interaction interfaces. To test this concept, we designed **osk6** to target the 6 nt long proximal stem of the spliced *oskar* localization element (SOLE, Figure 5A). This structure was demonstrated genetically to be essential for proper *oskar* mRNA localization by maintaining *oskar* mRNP motility.[23] When **osk6** was injected into *osk*MS2-mCherry-expressing oocytes, we could image the posterior

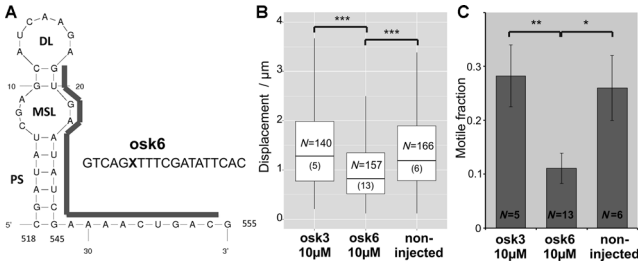

Figure 5. Effect of **osk6** on *oskar* mRNP motility. A) Predicted structure of the spliced *oskar* localization element and the target of **osk6**. B) Displacement and C) frequency of motile *oskar* mRNPs 60 min post injection. *** indicates $p < 0.001$ in a pair-wise Mann–Whitney test (D), * and ** indicates $p < 0.05$ and $p < 0.01$, respectively in two sample Student's t-test.

crescent of already localized *oskar* mRNA (Figure S6A). This indicates that the probe is able to hybridize with its target in vivo. The TO signal was not strong or contrasted enough for the detection of detect individual RNPs, as was also the case for **osk1d** (Movie S1) or **osk3** (Figure S6B) alone. However, the motility of *oskar* RNPs—tracked by using the mCherry signal—was strongly suppressed by the **osk6** probe: we observed significantly fewer and shorter runs during the imaging period (Figure 5B,C) than with the other probes. These findings are very similar to what was observed by Ghosh, Marchand, and colleagues upon disruption of SOLE secondary structure.[21]

In conclusion, we have developed a method that improves the brightness of fluorogenic hybridization probes (FIT probes) containing a single, environmentally sensitive thiazole orange (TO) nucleotide. The method relies on the introduction of an adjacent locked nucleic acid (LNA) unit, which induces a local constraint that closes decay channels for the TO excited state. The beneficial features—resistance against nuclease degradation, low fluorescence in the single-stranded state, very bright emission in the target-bound state—provided by LNA-enhanced gapmer FIT probes enabled the imaging of the dynamics of small, *oskar* mRNA containing ribonucleotide particles in developing *Drosophila melanogaster* oocytes. Signal-to-noise and signal-to-background ratios, as well as the measured RNP motility parameters are comparable to data obtained with a state-of-the-art transgenic detection system based on RNA tags and the expression of fluorescent MS2 coat fusion proteins. The FIT probes are the first fluorogenic hybridization probes that allow—in contrast to the study performed with molecular beacons by Mhlanga et al.[25]—the imaging of small RNPs of high motility. Based on this, we expect that LNA-enhanced gapmer FIT probes will find utility especially in the analysis of organisms where transgenic manipulation is not currently possible.

Received: June 8, 2014
Published online: August 28, 2014

Keywords: fluorescent probes · microscopy · mRNA · oligonucleotides · ribonucleoprotein particles

[1] a) T. T. Weil, R. M. Parton, I. Davis, *Trends Cell Biol.* **2010**, *20*, 380–390; b) V. Marchand, I. Gaspar, A. Ephrussi, *Curr. Opin. Cell Biol.* **2012**, *24*, 202–210.
[2] a) G. Bao, W. J. Rhee, A. Tsourkas, *Annu. Rev. Biomed. Eng.* **2009**, *11*, 25–47; b) S. Tyagi, *Nat. Methods* **2009**, *6*, 331–338.
[3] a) D. P. Bratu, B. J. Cha, M. M. Mhlanga, F. R. Kramer, S. Tyagi, *Proc. Natl. Acad. Sci. USA* **2003**, *100*, 13308–13313; b) Z. Pianowski, K. Gorska, L. Oswald, C. A. Merten, N. Winssinger, *J. Am. Chem. Soc.* **2009**, *131*, 6492–6497; c) R. M. Franzini, E. T. Kool, *J. Am. Chem. Soc.* **2009**, *131*, 16021–16023; d) H. Abe, J. Wang, K. Furukawa, K. Oki, M. Uda, S. Tsuneda, Y. Ito, *Bioconjugate Chem.* **2008**, *19*, 1219–1226; e) S. Kummer, A. Knoll, E. Socher, L. Bethge, A. Herrmann, O. Seitz, *Angew. Chem. Int. Ed.* **2011**, *50*, 1931–1934; *Angew. Chem.* **2011**, *123*, 1972–1975; f) S. Kummer, A. Knoll, E. Socher, L. Bethge, A. Herrmann, O. Seitz, *Bioconjugate Chem.* **2012**, *23*, 2051–2060; g) A. G. Torres, M. M. Fabani, E. Vigorito, D. Williams, N. Al-Obaidi, F. Wojciechowski, R. H. Hudson, O. Seitz, M. J. Gait, *Nucleic Acids Res.* **2012**, *40*, 2152–2167.
[4] a) B. A. Armitage, *Curr. Opin. Chem. Biol.* **2011**, *15*, 806–812; b) M. Baker, *Nat. Methods* **2012**, *9*, 787–790.
[5] E. Bertrand, P. Chartrand, M. Schaefer, S. M. Shenoy, R. H. Singer, R. M. Long, *Mol. Cell* **1998**, *2*, 437–445.
[6] S. Tyagi, F. R. Kramer, *Nat. Biotechnol.* **1996**, *14*, 303–308.
[7] J. J. Li, X. Fang, S. M. Schuster, W. Tan, *Angew. Chem. Int. Ed.* **2000**, *39*, 1049–1052; *Angew. Chem.* **2000**, *112*, 1091–1094.
[8] a) O. Seitz, F. Bergmann, D. Heindl, *Angew. Chem. Int. Ed.* **1999**, *38*, 2203–2206; *Angew. Chem.* **1999**, *111*, 2340–2343; b) O. Köhler, O. Seitz, *Chem. Commun.* **2003**, 2938–2939; c) O. Köhler, D. Venkatrao, D. V. Jarikote, O. Seitz, *ChemBioChem* **2005**, *6*, 69–77; d) E. Socher, L. Bethge, A. Knoll, N. Jungnick, A. Herrmann, O. Seitz, *Angew. Chem. Int. Ed.* **2008**, *47*, 9555–9559; *Angew. Chem.* **2008**, *120*, 9697–9701.
[9] a) L. Bethge, I. Singh, O. Seitz, *Org. Biomol. Chem.* **2010**, *8*, 2439–2448; b) F. Hövelmann, L. Bethge, O. Seitz, *ChemBioChem* **2012**, *13*, 2072–2081.
[10] F. Hövelmann, I. Gaspar, A. Ephrussi, O. Seitz, *J. Am. Chem. Soc.* **2013**, *135*, 19025–19032.
[11] a) V. Karunakaran, J. L. Perez Lustres, L. Zhao, N. P. Ernsting, O. Seitz, *J. Am. Chem. Soc.* **2006**, *128*, 2954–2962; b) L. G. Lee, C.-H. Chen, L. A. Chiu, *Cytometry* **1986**, *7*, 508–517; c) J. Nygren, N. Svanvik, M. Kubista, *Biopolymers* **1998**, *46*, 39–51.
[12] a) G. L. Silva, V. Ediz, D. Yaron, B. A. Armitage, *J. Am. Chem. Soc.* **2007**, *129*, 5710–5718; b) A. Sanchez-Galvez, P. Hunt, M. A. Robb, M. Olivucci, T. Vreven, H. B. Schlegel, *J. Am. Chem. Soc.* **2000**, *122*, 2911–2924; c) A. Yartsev, J.-L. Alvarez, U. Åberg, V. Sundström, *Chem. Phys. Lett.* **1995**, *243*, 281–289.
[13] M. Petersen, K. Bondensgaard, J. Wengel, J. P. Jacobsen, *J. Am. Chem. Soc.* **2002**, *124*, 5974–5982.
[14] a) K. E. Nielsen, S. K. Singh, J. Wengel, J. P. Jacobsen, *Bioconjugate Chem.* **2000**, *11*, 228–238; b) M. Petersen, C. B. Nielsen, K. E. Nielsen, G. A. Jensen, K. Bondensgaard, S. K. Singh, V. K. Rajwanshi, A. A. Koshkin, B. M. Dahl, J. Wengel, J. P. Jacobsen, *J. Mol. Recognit.* **2000**, *13*, 44–53; c) K. E. Nielsen, J. Rasmussen, R. Kumar, J. Wengel, J. P. Jacobsen, M. Petersen, *Bioconjugate Chem.* **2004**, *15*, 449–457.
[15] a) A. Ivanova, G. Jezierski, N. Rosch, *Phys. Chem. Chem. Phys.* **2008**, *10*, 414–421; b) A. Ivanova, N. Rosch, *J. Phys. Chem. A* **2007**, *111*, 9307–9319.
[16] U. Wenge, J. Wengel, H.-A. Wagenknecht, *Angew. Chem. Int. Ed.* **2012**, *51*, 10026–10029; *Angew. Chem.* **2012**, *124*, 10168–10172.
[17] a) S. Obika, D. Nanbu, Y. Hari, J. Andoh, K. Morio, T. Doi, T. Imanishi, *Tetrahedron Lett.* **1998**, *39*, 5401–5404; b) A. A. Koshkin, P. Nielsen, M. Meldgaard, V. K. Rajwanshi, S. K. Singh, J. Wengel, *J. Am. Chem. Soc.* **1998**, *120*, 13252–13253.

[18] D. V. Jarikote, N. Krebs, S. Tannert, B. Röder, O. Seitz, *Chem. Eur. J.* **2007**, *13*, 300 – 310.
[19] a) A. Ephrussi, L. K. Dickinson, R. Lehmann, *Cell* **1991**, *66*, 37 – 50; b) J. Kim-Ha, J. L. Smith, P. M. Macdonald, *Cell* **1991**, *66*, 23 – 35.
[20] V. L. Zimyanin, K. Belaya, J. Pecreaux, M. J. Gilchrist, A. Clark, I. Davis, D. St. Johnston, *Cell* **2008**, *134*, 843 – 853.
[21] a) H. Jambor, C. Brunel, A. Ephrussi, *RNA* **2011**, *17*, 2049 – 2057; b) M. Chekulaeva, M. W. Hentze, A. Ephrussi, *Cell* **2006**, *124*, 521 – 533.
[22] Although the signal-to-noise ratio of particles detected by this FIT probe mixture remained comparable (Figure 4B), the raw brightness (Figure 4A and A″) was substantially lower than that of the oskMS2–GFP system (Figure 3A and A″).
[23] S. Ghosh, V. Marchand, I. Gaspar, A. Ephrussi, *Nat. Struct. Mol. Biol.* **2012**, *19*, 441 – 449.
[24] The image quality obtained was somewhat inferior to that of the oskMS2–GFP system, especially concerning background (see e.g. Figure 4E; Figure S3E and Figure S4C). This was not unexpected since MCP–GFP molecules not binding to target RNA are sequestered in the nucleus of the cells, whereas the injected probes are expected to fill the oocyte homogenously.
[25] M. M. Mhlanga, D. P. Bratu, A. Genovesio, A. Rybarska, N. Chenouard, U. Nehrbass, J. C. Olivo-Marin, *PloS one* **2009**, *4*, e6241.
[26] Y. Shimada, K. M. Burn, R. Niwa, L. Cooley, *Dev. Biol.* **2011**, *355*, 250 – 262.

